HNPS Advances in Nuclear Physics

Vol 28 (2021)

HNPS2021

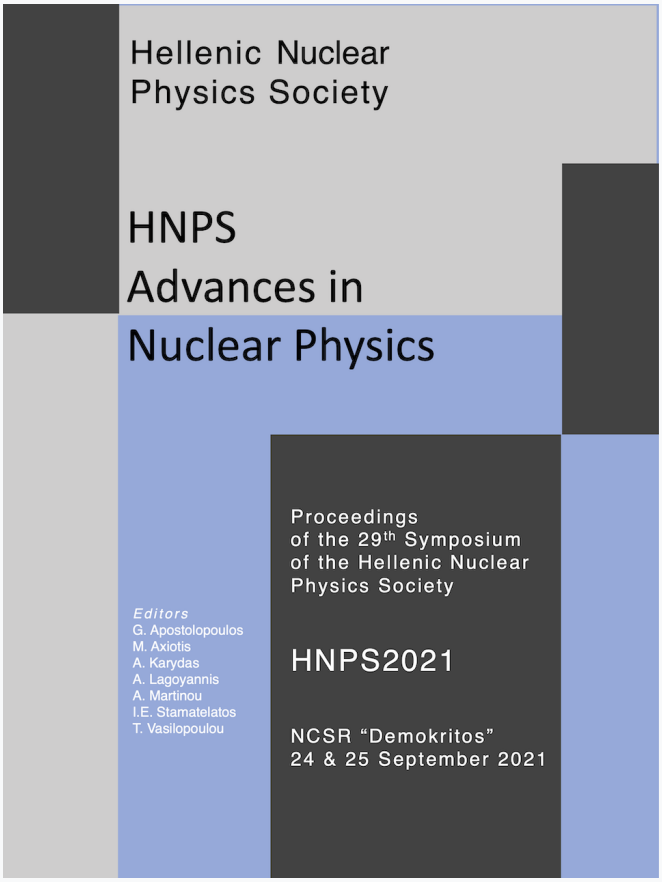

Advances in Cosmic Ray Muon Computed Tomography and Fieldable Spectroscopy

Stylianos Chatzidakis, Junghyun Bae

doi: 10.12681/hnps.3584

To cite this article:

Chatzidakis, S., & Bae, J. (2022). Advances in Cosmic Ray Muon Computed Tomography and Fieldable Spectroscopy. *HNPS Advances in Nuclear Physics*, *28*, 184–190. https://doi.org/10.12681/hnps.3584

Advances in Cosmic Ray Muon Computed Tomography and Fieldable Spectroscopy

S. Chatzidakis[1,*] and J. Bae[1]

[1] *School of Nuclear Engineering, Purdue University, IN 47906*

Abstract A recent example of successful technology transition from high energy physics to practical engineering applications is cosmic ray muon tomography. Cosmic ray muon tomography, is a promising non-destructive technique that has been recently utilized to monitor or image the contents of dense or well shielded objects, typically not feasible with conventional radiography techniques, e.g., x-ray or neutron. Cosmic ray muon tomography has been used with various levels of success in spent nuclear fuel monitoring, volcano imaging, and cargo container imaging. Further, knowledge of cosmic ray muon momentum spectrum has the potential to significantly improve and expand the use of a variety of recently developed muon-based radiographic techniques. However, existing muon tomography systems rely only on muon tracking and have no momentum measurement capabilities which reduces the image resolution and requires longer measurement times. A fieldable cosmic ray muon spectrometer with momentum measurement capabilities for use in muon tomography is currently missing. In this paper, we will discuss and explore recent advances in cosmic ray muon computed tomography and spectroscopy and their applications to engineering including a new concept for measuring muon momentum using multiple gaseous Cherenkov radiators. By varying the pressure of multiple gas Cherenkov radiators, a set of muon momentum threshold levels can be selected that are triggered only when the incoming muon momentum exceeds that level. As a result, depending on the incoming muon momentum, none to all Cherenkov radiators can be triggered. By analyzing the signals from each radiator, we can estimate the actual muon momentum.

Keywords cosmic ray muons, muon tomography, muon momentum

INTRODUCTION

Cosmic ray muons are charged particles, having approximately 200 times the mass of electron, generated naturally in the atmosphere, and rain down upon the earth at an approximate rate of 10,000 particles m^{-2} min^{-1} [1]. While the existence of cosmic muons and the theory which describes their transport and Multiple Coulomb Scattering (MCS) in matter is well understood it is only recently that the applicability of muons for imaging has been investigated [2]. Monitoring shielded containers, e.g., cargo containers or spent fuel dry casks, or large facilities, e.g., reactors, using cosmic ray muons has the potential to allow for non-destructive assessment of stored contents, investigate whether the stored content agrees with the declared content, minimize the risks of nuclear proliferation and reduce potential homeland threats [3]. Conventional radiographic methods for examining the interior of containers, e.g., photons, with a mean free path approximately in the order of 25 g/cm^2 results to less than 2 cm penetration

* Corresponding author, email: schatzid@purdue.edu

in lead, are limited [4]. Increasing the photon energy does not increase penetrating distance due to an increase in pair production phenomena. Similarly, electrons cannot penetrate far into matter due to large momentum transfers and radiation emission (Bremsstrahlung). For example, 1 GeV electrons can penetrate water only within 1 m and commercially available portable Betatrons can generate electron with energies less than 10 MeV. Protons have been shown to penetrate several meters in dense materials and their potential has been demonstrated for large object imaging [5]. However, production of such high-energy protons requires large, expensive and immovable accelerators. A non-conventional class of ionizing particles, cosmic ray muons, present certain advantages over the previously mentioned ionizing radiation. Muons have the ability to penetrate high density materials and their range increases with increasing energy. Figure 1 shows the range of 1 GeV muons as a function of atomic number and the range of muons as a function of energy. With the exception of protons, muons have the largest penetrating capabilities even in dense materials such as uranium and lead. In addition, muons are freely available and no radiological sources are required resulting in a total absence of any artificial radiological dose.

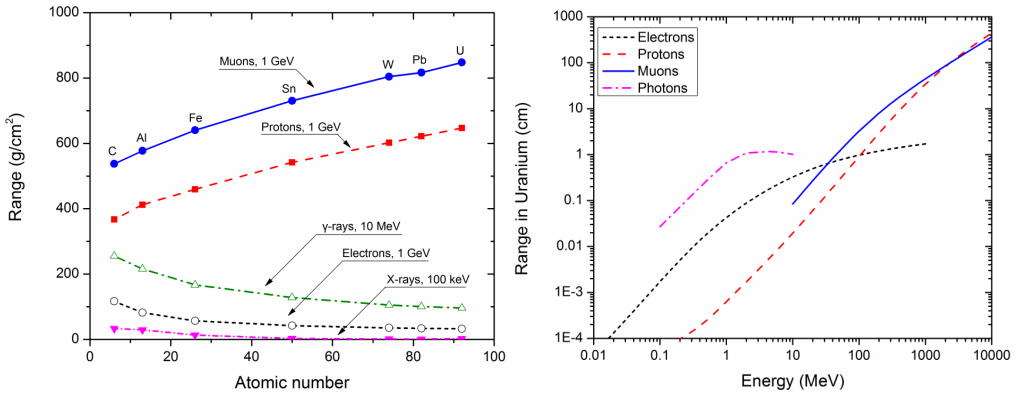

Fig. 1. Range (mass density units) of various radiation types in various materials (left). Range in (cm) uranium as a function of energy (right).

MUON DETECTORS

Several detector types have been proposed for muon detection in monitoring and imaging applications. These include scintillators, drift tubes, resistive plate chambers and, solid state detectors. Cox et al. [3] summarized the requirements for muon detector development concluding that coincidence timing in the order of nanoseconds, spatial resolution in the order of sub-mm and energy determination will be required for future applications. They noted that efficient detectors with large area and sensitivity over hundreds of GeV would be needed to optimize statistics and reduce the time taken to collect adequate number of muons. Increasing detector separation distance decreases solid angle and increases detector volume. A time of flight technique was proposed for extracting energy information. It was concluded that picosecond timing resolution would be required to differentiate between sub-GeV and GeV muon energies.

Existing muon detectors have used drift-wire chambers, e.g., the Large Muon Tracker

developed at Los Alamos National Laboratory (LANL) with 6 top and 6 bottom planes, sampling area 2.0x2.0 m^2, consisting of drift tube chambers and scintillator paddles for triggering [6]. A similar smaller prototype designed to be transportable is the Mini Muon Tracker with 576 drift tubes in total, 2 super-modules, 6 planes of drift tubes each, active area 1.2x1.2 m^2, sampling area 100x100x60 cm^3, and resolution 400 μm (2 mrad) [7]. Delay line chambers have also been used for demonstration at LANL consisting of four drift chambers, active area 60x60 cm^2, sampling area 27 cm, and precision 400 μm FWHM [8]. A small prototype with gas electron multiplier detectors has been developed by the HEP laboratory at Florida Tech to determine muon positional information [9]. The Muon Portal developed by INFN [10] consists of four planes of plastic scintillator strips spaced 1.4 m apart 3x6 m^2, sampling area 2.8 m, and resolution 3.5 mm (0.2 degrees). Another prototype by INFN includes drift wire chambers, a sampling area of 160 cm height and 11 m^3 volume, an active area of 3x2.5 m^2, achieving a resolution in the order of 200 μm [11]. A large prototype having 1,452 plastic scintillator strips, active area 2.0x2.0 m^2, sampling area 2.0 m (1.6x2.0x2.0 m^3), resolution 2.3-3.4 mm and muon spectrometer was developed by the CRIPT collaboration [12]. Resistive plate chambers have been explored as muon detectors and a prototype having 12 glass RPCs with 2 mm gas gap, layer spacing 90 mm, sensitive area 500x500 mm^2 and intrinsic spatial resolution 300-900 μm exists [13]. Finally, a large prototype consisting of 24 glass RPCs with sampling area 1800x600 mm^2 and spatial resolution 150-500 μm is under development. Table 1 provides a summary of existing muon detectors.

Table 1. Main characteristics of muon detector prototypes.

	Detector type	Active area	Sampling volume	Resolution	Efficiency
LANL prototype [8]	Delay line readout multiple wire drift chambers	60x60 cm^2	60x60x27 cm^3	400 μm	>96%
Mini Muon Tracker [7]	Drift wire chambers	1.2x1.2 m^2	100x100x60 cm^3	400 μm (2 mrad)	>90%
Large Muon Tracker [6]	Drift wire chambers	2.0x2.0 m^2	2.0x2.0x1.5 m^3	400 μm (2 mrad)	>96%
Muon Portal INFN [10]	Plastic scintillator strips	3x6 m^2	3x6x2.8 m^3	3.5 mm (3.5 mrad)	>90%
INFN [11]	Drift wire chambers	3x2.5 m^2	3 x 2.5x1.6 m^3	200 μm	>90%
CRIPT [12]	Plastic scintillator bars	2.0x2.0 m^2	1.6x2.0x2.0 m^3	3 mm (6 mrad)	>99.5%
RPC [13]	Resistive plate chambers	0.5x0.5 m^2	0.09x0.5x0.5 m^3	300-900 μm	>95%

MUON TOMOGRAPHY

Early efforts have mainly focused on the use of muons for cargo scanning applications and proof of principle studies [14-17]. It was pointed out that muon attenuation and scattering has several advantages over traditional methods and muon imaging would be better suited for large containers storing unknown materials. Osterlund et al. (2006) investigated the possibility to detect missing fuel assemblies in copper canisters used for disposition of spent nuclear fuel using simulated muon data corresponding to 15 minutes of measurement time [14]. Jonkmans et al. (2013) performed simulations aiming to identify four missing columns of CANDU type fuel assemblies in dry storage containers [15]. It was demonstrated using simulated muon data equivalent to 1 day of measurement that the sensitivity of the method is adequate and exceeds the IAEA detection target for non-proliferation requirements. Simulations and the development of a small scale prototype to discriminate between low and high-Z materials stored in a small concrete barrel were performed by Clarkson et al (2014) [16]. Using data collected equivalent to 30 weeks of measurements and voxel size 5x5x10 mm^3 were able to identify uranium and tungsten objects within concrete barrel. Similarly, Thomay et al. (2016) used muon scattering tomography to obtain 3D images of the contents of legacy nuclear waste drums [17]. High and low density materials enclosed in concrete were resolved, for example a small tungsten cylinder and a thin uranium sheet were identified. A notable example is the experimental effort by Durham et al. (2016) which used a small muon prototype, the Mini Muon Tracker, to identify missing PWR fuel bundles from a sealed vertical dry cask [7]. They performed measurements on a partially loaded vertical dry storage cask and were able to reconstruct 2D images of areal density and locate columns of missing fuel bundles but not the exact location. Muon data collected for 200 hours resulting in ~10^5 muons. They proposed the rotation of the detector around the cask to obtain data from several viewing angles.

The GEANT4 (GEometry ANd Tracking) Monte Carlo code [18-20] is typically used to perform muon transport simulations and estimate muon paths through large objects, e.g., spent nuclear fuel dry casks. As schematically shown in Figure 2, GEANT4 requires parameters related to object geometry, muon energy, and angular distributions. However, GEANT4 does not provide a built in library with muon energy and angular distributions. To generate muons from the actual measured muon spectrum a cosmic ray muon sampling capability, e.g., a "Muon Event Generator" [21], is needed. The "Muon Event Generator" is based on a phenomenological model that captures the main characteristics of the experimentally measured spectrum coupled with a set of statistical algorithms. The muons generated can have zenith angles in the range 0-90^o and energies in the range 1-100 GeV. The muon angular and energy distributions are reproduced and integrated into GEANT4. The "Muon Event Generator" offers a way to allow easy coupling with GEANT4 interface. It generates the necessary user-defined histograms for use with the GEANT4 G4GeneralParticleSource macro file.

Muon detection and scattering measurement requires placement of detectors on two opposite sides of the object to be inspected. The detectors are modeled as parallel planes of position sensitive chambers, e.g., drift-wire chambers or gas-electron multiplier detectors, which record the position of each muon before and after interaction with the dry cask. Each muon will result

in four recorded position measurements. Only muons that pass through all detector planes were recorded. Cosmic ray muons pass through the first detector plane, i.e., farthest detector plane through which a muon passes, and their initial positions are recorded. The muons then pass through the object before hitting and interacting with the second plane of detectors where their final positions are also recorded. This information is then processed using monitoring, classification and imaging algorithms [22-27].

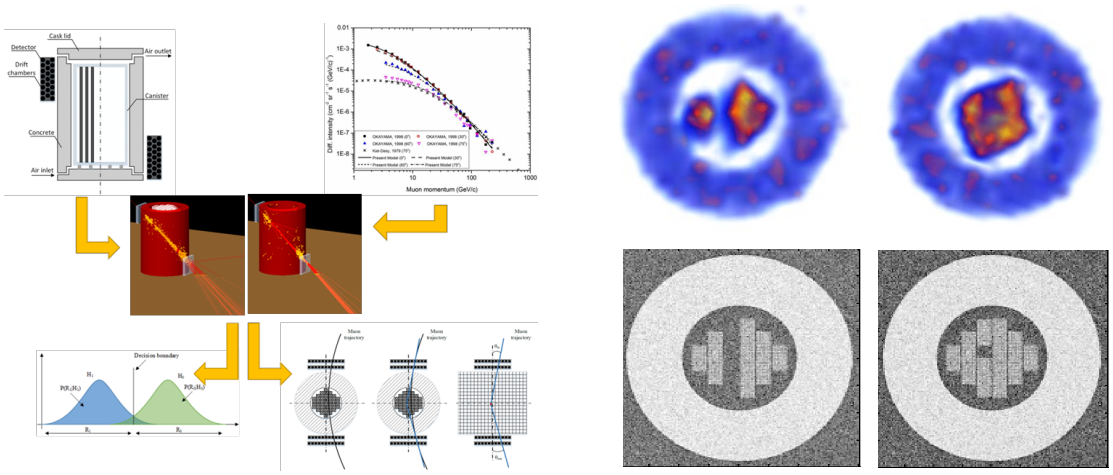

Fig. 2. GEANT4 model construction (left) and 2D reconstruction using two different imaging algorithms (right) [22-27].

MUON SPECTROMETERS

Despite the potential and success, the wide application of cosmic ray muons is limited by the naturally low muon intensity. Since it is not practicable to deploy accelerators in the field to provide muon beams, it is important to measure muon momentum to maximize the utilizability of each cosmic ray muon. However, it is still challenging to measure muon momentum in the field without resorting to large solenoid or toroid magnets, or other specialized instruments, e.g., Cherenkov ring imagers, or time-of-flight detectors [27-29]. At present, no portable detector exists that can measure muon momentum in the field.

A new approach to measure muon momentum has been recently proposed using coupled pressurized gaseous Cherenkov radiators. Unlike solid or liquid Cherenkov radiators, the refractive index of gas radiators can be changed by varying gas pressure and temperature. As a result, the necessary muon threshold momentum levels by carefully selecting the gas pressure at each radiator. By measuring the Cherenkov signals in each radiator, the muon momentum can then be estimated. Geant4 simulation results demonstrate that such a system can measure muon momentum with a high accuracy level (> 85%) and with a resolution of 0.5 GeV/c. The benefits of such a spectrometer are that it is compact and portable enough so that it can be deployed in many fields to solely measure muon momentum or be coupled with the existing systems such as off-site underground particle experiment laboratory, i.e., underground laboratories, or in the space for the cosmic radiation measurement, i.e., international space station.

The underlying principle of the proposed muon spectrometer is illustrated in Figure 3. It shows the characteristics of photon emissions by Cherenkov, scintillation, and transition radiation in Radiator A ($p_\mu > p_{th}$) and B ($p_\mu < p_{th}$). All surfaces of gas radiator tanks are wrapped by a strong photon absorber so that emitted photons are isolated within the radiators and optical sensors are installed on one side of each radiator tank to measure photon signals. In this way, scintillation photons can be discriminated from the Cherenkov photon signals because scintillation photons are emitted in all directions whereas Cherenkov photons are emitted forward-biased directions. In addition, two scintillation plates are used for a two-fold coincidence so that muon signals are efficiently discriminated from background radiation. A visualization of the spectrometer in GEANT4 that highlights the emitted Cherenkov photons from a 10 GeV muon is shown in Figure 3.

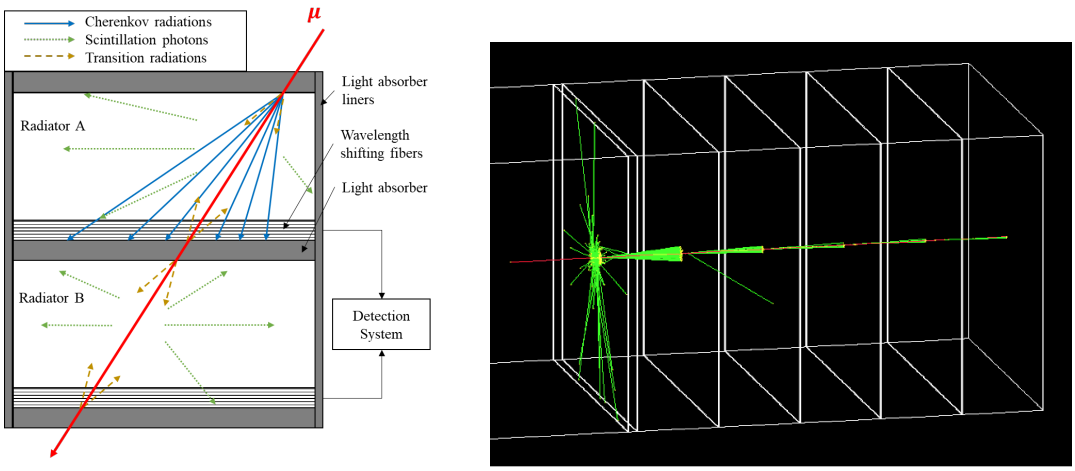

Fig. 3. Concept of a gas Cherenkov muon spectrometer (left) and visualization in GEANT4 (right) [28, 29].

SUMMARY

Cosmic ray muons are relativistic particles with energies in the order of GeV that can play an important role in non-proliferation and monitoring applications presenting unique advantages over existing methods. Research on muon detectors and imaging approaches for real time monitoring and imaging of large objects using muon scattering, displacement, and transmission are constantly improving and expanding this field. It is worth noting that recent studies show that one missing fuel assembly could be distinguished from a fully loaded cask with a small overlapping between the distributions when more than $3x10^5$ muons are measured and muon momentum information is included in the reconstruction. This indicates that the removal of a standard fuel assembly could be identified using muons providing that enough muons are collected. The increasing separation of the distributions reveals that the scattering variance can be used as a feature for discrimination between casks and the development of a classifier for that purpose is possible.

References

[1] K. Hagiwara et al., Phys. Rev. D, 66, pp. 1-974 (2002)
[2] P.M. Jenneson, Nucl. Instr. Methods Phys. Res. A 525, pp. 346-351 (2004)
[3] L. Cox, Nat. Nucl. Sec. Div., AWE, UK (2010)
[4] K.N. Borozdin et al., Nature 422, p. 277 (2003)
[5] J. Gustafsson, Diploma thesis, Uppsala University, Sweden (2005)
[6] J.A. Green et al., IEEE Nucl. Sci. Symp. Conf. Rec., 1-6, pp. 285-288 (2006)
[7] J.M. Durham et al., J. Nuc. Mat. Manag., vol. 44, 3 (2016)
[8] L.J. Schultz, Thesis dissertation, Portland State University (2003)
[9] R.C. Hoch, M.S. thesis, Florida Institute of Technology (2009)
[10] S. Pesente, S. et al., Nuclear. Instr. Methods. Phys. Res. A 604, pp. 738-746 (2009)
[11] E. Astrom et al., J. Inst., vol. 11, P07010 (2016)
[12] V. Anghel et al., Nuclear. Instr. Methods. Phys. Res. A 798, pp. 12-23 (2015)
[13] P. Baesso et al., J. Inst., vol 9, C10041 (2014)
[14] M. Osterlund et al., Int. Workshop on Fast Neutron Det. and Appl. (2006)
[15] G. Jonkmans et al., Ann. Nuc. Ene., 53, pp. 267-273 (2013)
[16] A. Clarkson et al., 4th Int. Conf. on Adv. in Nucl. Instr. Measurem. Methods and Appl. (2015)
[17] C. Thomay et al., J. Inst., 11, P03008 (2016)
[18] S. Agostinelli et al., Nucl. Instr. Methods Phys. Res. A, 506, pp. 250–303 (2003)
[19] J. Allison et al., IEEE Transactions on Nuclear Science, 53(1) pp. 270-278 (2006)
[20] A.G. Bogdanov et al. IEEE Trans. Nucl. Sci., 53(2) pp. 513-519 (2006)
[21] S. Chatzidakis et al., Nucl. Instr. Methods Phys. Res. A 804, pp. 33-42 (2015)
[22] Z. Liu et al., IEEE Trans. Imag. Process., 28, Issue 1, pp 426-435 (2018)
[23] S. Chatzidakis et al., J. of Appl. Phys. 123, 124903 (2018)
[24] S. Chatzidakis et al., Nucl. Instr. Methods Phys. Res. A 828, pp. 37-45 (2016)
[25] S. Chatzidakis et al., Nucl. Plant Instrum., Contr. Interf. Technol., pp. 237–245 (2017)
[26] S. Chatzidakis et al., IEEE Trans. Nucl. Sci. 63, pp. 2866–2874 (2016)
[27] S. Chatzidakis et al., ANS Annual Meeting 116, pp. 190–193, (2017)
[28] J. Bae and S. Chatzidakis, INMM/ESARDA (2021)
[29] J. Bae and S. Chatzidakis, IEEE Nucl. Sci. Symp. Med. Imag. Conf. (2021)